J Neuropathol Exp Neurol
Vol. , No. , , pp. 1–8
https://doi.org/10.1093/jnen/nlac075

OXFORD

ORIGINAL ARTICLE

Clinical, Pathological, and Molecular Characteristics of Diffuse Spinal Cord Gliomas

Mekka R. Garcia, MD, Yang Feng, PhD, Varshini Vasudevaraja, MS, Kristyn Galbraith, MD, Jonathan Serrano, MS, Cheddhi Thomas, MD, Alireza Radmanesh, MD, Eveline T. Hidalgo, MD, David H. Harter, MD, Jeffrey C. Allen, MD, Sharon L. Gardner, MD, Diana S. Osorio, MD, Christopher M. William, MD, PhD, David Zagzag, MD, PhD, Daniel R. Boué, MD, PhD, and Matija Snuderl, MD

Abstract

Diffuse spinal cord gliomas (SCGs) are rare tumors associated with a high morbidity and mortality that affect both pediatric and adult populations. In this retrospective study, we sought to characterize the clinical, pathological, and molecular features of diffuse SCG in 22 patients with histological and molecular analyses. The median age of our cohort was 23.64 years (range 1–82) and the overall median survival was 397 days. K27M mutation was significantly more prevalent in males compared to females. Gross total resection and chemotherapy were associated with improved survival, compared to biopsy and no chemotherapy. While there was no association between tumor grade, K27M status ($p = 0.366$) or radiation ($p = 0.772$), and survival, males showed a trend toward shorter survival. K27M mutant tumors showed increased chromosomal instability and a distinct DNA methylation signature.

Key Words: Gliomas, H3-K27M, Molecular, Neuro-oncology, Spinal cord, Tumors.

Department of Neurology, NYU Langone Health, New York, New York, USA (MRG, JCA); Department of Biostatistics, NYU School of Global Public Health, New York, New York, USA (YF); Department of Pathology, NYU Langone Health, New York, New York, USA (VV, KG, JS, CT, CMW, DZ, MS); Department of Radiology, NYU Langone Health, New York, New York, USA (AR); Department of Neurosurgery, NYU Langone Health, New York, New York, USA (ETH, DHH); Department of Pediatrics, NYU Langone Health, New York, New York, USA (SLG); Department of Pediatrics, Nationwide Children's Hospital, Columbus, Ohio, USA (DSO); and Department of Pathology and Laboratory Medicine, Nationwide Children's Hospital and the Ohio State University, Columbus, Ohio, USA (DRB).

Send correspondence to: Matija Snuderl, MD, Department of Pathology, NYU Langone Health, 240 E. 38th Street, 22nd Floor, New York, NY 10016, USA; E-mail: matija.snuderl@nyulangone.org

The authors have no duality or conflicts of interest to declare.

INTRODUCTION

Primary spinal cord tumors are rare, with an overall incidence of approximately 0.22 per 100 000 and account for 2%–4% of all central nervous system tumors (1–3). Spinal cord gliomas (SCGs) represent 8%–10% of primary spinal cord tumors of which the majority are intramedullary and histologically classified as astrocytomas and ependymomas (4, 5). Astrocytomas could be further subdivided depending on histology, with low-grade pilocytic astrocytoma accounting for most SCG, while infiltrating gliomas can be challenging to grade on histology alone as samples are usually small given the morbidity associated with surgical biopsy and/or resection. The current treatment of SCGs is maximal safe surgical resection followed by an adjuvant chemotherapy and/or radiation based on regimens designed for other brain tumors with similar histology; usually with poor outcomes (6, 7). However, limited understanding of SCG biology impairs our ability to improve the treatment of this disease. Furthermore, though histologically similar to their intracranial counterparts, diffuse SCGs have distinct genetic alterations and molecular profiles (8, 9).

Recent genome-wide studies have established molecular drivers in intracranial gliomas and have revealed distinct genomic aberrations. The discovery of recurrent mutations in isocitrate dehydrogenase 1 and 2 (*IDH1/2*) and the *H3F3A* and *HIST1H3B* genes encoding the histone H3 variants H3.3 and H3.1, respectively, are important genetic drivers of diffuse gliomas in both children and adults (10, 11). Tumors with G34R/G34V mutations arise in the cerebral hemispheres, while K27-altered tumors are classically present in midline brain structures, such as the thalamus, hypothalamus, brainstem, and spinal cord (12, 13). These midline tumors harboring the K27M mutation are thought to primarily occur in children and young adults and are associated with a very poor prognosis. While K27-altered cerebral tumors have been the focus of multiple studies over the years, characteristics of K27-altered SCGs are less well-explored largely due to their rarity.

We have previously shown the usefulness of genome-wide DNA methylation in defining the molecular signatures

© The Author(s) 2022. Published by Oxford University Press on behalf of American Association of Neuropathologists, Inc.
All rights reserved. For permissions, please email: journals.permissions@oup.com

Downloaded from https://academic.oup.com/jnen/advance-article/doi/10.1093/jnen/nlac075/6673886 by New York Universtiy Law School Library user on 15 September 2022

of rare tumors, such as pleomorphic xanthoastrocytomas (14). Few studies to date have examined genome-wide DNA methylation in diffuse SCG. In addition to the DNA methylation-based classification, DNA methylation array also enables the assessment of the copy number profile. Due to the limited quantities of spinal cord biopsy samples, separate large DNA NGS panels or genomic array for copy number assessment are often not feasible. Here, we present a large cohort of primary diffuse SCG. Incorporating the utility of genome-wide DNA methylation analysis, we retrospectively analyzed the clinical, pathological, and molecular features of 22 pediatric and adult patients with diffuse SCG. We reviewed clinical data, histology and H3 K27M mutation status, and molecular features and copy number of each tumor by DNA methylation.

MATERIALS AND METHODS

Patients and Clinical Data

Histopathological analyses and medical chart reviews were performed on patients diagnosed with intramedullary diffuse glioma histological World Health Organization (WHO) Grade 2–4 at NYU Langone Medical Center and Nationwide Children's Hospital between 1998 and 2018. Pediatric patients were defined as <18 years of age and adult as ≥18 years of age. All tumors were primary, originating in the spinal cord. Patients with a histological diagnosis of ependymoma and pilocytic astrocytoma were excluded from this study. Clinical presentation, neuroimaging features, extent of surgery, adjuvant therapy, and follow-up were recorded from patients' medical records. Approval from the institutional review board was obtained before the initiation of this study (NYU IRB #i14-00948). A gross total resection (GTR) was defined as a complete removal of all tumors based on either the surgeons' notes after completion of the procedure or a magnetic resonance imaging (MRI) exam that demonstrated no residual tumor, subtotal resection was defined as resection with residual tumor. In biopsies, only a representative sample was provided for diagnosis and a resection was not attempted per surgeon's notes. Disease progression was defined as either a new lesion that appeared after initial treatment (surgery, radiation, and/or chemotherapy), or as the enlargement of an existing lesion after subtotal resection/biopsy and adjuvant therapy.

Histology and Immunohistochemistry

Tissue samples for all analyses were obtained from the initial surgery. Formalin-fixed paraffin-embedded (FFPE) sections were stained by the hematoxylin and eosin method from all tumor blocks and were reviewed and histologically graded independently by 2 neuropathologists (MS and CT) using WHO 2021 criteria. In cases of inter-observer disagreement, the case was reviewed together and the final grade was established as a consensus of both observers. Representative paraffin blocks from each tumor were selected for immunohistochemistry (IHC) analysis. Mutation-specific IHC for histone H3 K27M, IDH1-R132H, and BRAF V600E was performed in the CLIA-certified pathology clinical IHC laboratory following established clinical protocols.

Radiological Analysis

Of the 22 patients, preoperative brain MRI from 16 patients with glioblastoma, IDH-wildtype, astrocytoma IDH-wildtype, diffuse midline glioma, H3 K27-mutant diagnosed by histology and/or methylation was available. A board-certified pediatric neuroradiologist reviewed all magnetic resonance images. Each tumor was evaluated for enhancement, edema, and leptomeningeal dissemination.

Whole-Genome DNA Methylation Profiling

Genome-wide methylation was possible in 16/22 patients. DNA was extracted from the FFPE tissue using the automated Maxwell system following clinically validated protocol (Promega, Madison, WI). The DNA methylation kit from Zymo Research (Irvine, CA) was then used to bisulfite-convert the DNA samples. Whole-genome DNA methylation analysis and classification were performed at the NYU Molecular Laboratory as described previously using the Illumina methylation array. The raw IDATs image files were generated from iScan, processed and analyzed using the Bioconductor R Minfi package (15). The samples were profiled with different array types (450K and EPIC). The CpG probes that were common between 2 array types were obtained using combineArrays from the Minfi package. The probes were then quantile normalized and corrected for background signal. Samples were then checked for their quality by calculating the mean detection p value. Samples with p values <0.05 were used for further analysis. dbSNP and sex chromosome probes were excluded from analysis to rule out any variation in the downstream analysis. Beta values were generated using the resulting set of probes. Differential methylation analysis was done comparing K27M versus Wt samples which resulted in 84 probes that were significant (false disscover rate [FDR] < 0.05). Beta values <0.2 were considered as hypomethylated probes and probes with beta value >0.8 were considered hypermethylated. Heatmaps were generated in a semi-supervised manner using the ComplexHeatmap R package, which shows the hierarchical clustering between the samples for top 84 significantly differentially methylated probes along with tumor grade, sex, K27M status, histology, and spinal tumor location annotations (16).

Copy Number Variation Analysis

DNA methylation array data profiled on 16/22 samples were also used to perform the copy number variation (CNV) using the conumee R package (17). Each sample was processed using conumee to generate CNV segment files which were then combined to generate a CNV Summary plot between K27M and wildtype samples. Frequency of copy number gains and losses were generated using the GenVisR package between K27M versus wildtype sample types (18). Green represents copy number gains and red represents copy number loss.

Statistics

Clinical and pathological variables were compared using 2-tailed Fisher exact test, Chi-squared statistics, and

Downloaded from https://academic.oup.com/jnen/advance-article/doi/10.1093/jnen/nlac075/6673886 by New York University Law School Library user on 15 September 2022

Wilcoxon rank sum test with continuity correction. Survival analysis was performed using the log-rank test and Kaplan-Meier method to compare different groups. Overall survival was defined as the time from the initial surgery to death. P values <0.05 were considered statistically significant. RStudio software was used for analysis.

RESULTS

Clinicopathological Characteristics

The clinical characteristics of our cohort are summarized in the Table. The median age was 23.64 years (range 1–82 years). There was a significant male predominance for the K27M-mutant tumors compared to H3-wildtype ($p < 0.05$). Tumor location distribution was divided between cervical (50%), thoracic (41%), and lumbar (10%). There was a significant predilection toward the thoracic region for pediatric patients compared to adults ($p = 0.03$). One pediatric patient developed metastasis to the pons at the time of progression. Only 17 patients had complete clinical data for survival analysis, with the median overall survival of 397 days (Fig. 1). There was a trend of decreased overall survival when comparing male versus female patients ($p = 0.06$). However, histological tumor grade or H3 K27M mutation status showed no significant association with overall survival ($p = 0.779$) and ($p = 0.366$), respectively.

Of the patients with data available, GTR was achieved in 5 (23%) cases, while most patients (55%) underwent subtotal resection or a biopsy. Biopsy was associated with overall decreased survival compared to GTR ($p = 0.022$) (Fig. 1). Ten patients received adjuvant radiotherapy (45%), 11 chemotherapy (50%), and 9 radiotherapy/chemotherapy (41%). More patients with K27M-mutant tumors received adjuvant radiotherapy ($p = 0.07$), chemotherapy ($p = 0.03$), and radiotherapy/chemotherapy combined ($p = 0.02$) compared to patients with H3-wildtype tumors. Patients who did not receive chemotherapy had an overall decreased survival compared to those who received chemotherapy ($p = 0.019$), while radiotherapy was not associated with significant improvement in overall survival ($p = 0.772$). The percentage of patients with H3-wildtype tumors receiving adjuvant radiotherapy (22%), chemotherapy (22%), and both radiotherapy/chemotherapy (11%) was lower than that of H3 K27M-mutant tumor patients (62%, 69%, and 62%, respectively with $p = 0.07$, $p = 0.03$, and $p = 0.02$). Of the 2H3-wildtype patients who received radiation, one received only one round. Other therapeutic agents included intravenous immunogobulin (IVIG), nivolumab, avastin, crizotinib, binimetinib, zarnestra, temozolomide, vinblastine, trametinib, everolimus, and ONC201.

TABLE. Patient Demographics

Variable	WT (n = 9)	H3 K27M (n = 13)	p Value
Age (years)	28.7 ± 29.75	20.2 ± 15.7	0.39
Sex (male)	2 (22)	9 (90)	0.02
WHO tumor grade	2.75 ± 0.81	3.9 ± 0.27	<0.0001
2	5 (55.5)	0 (0)	0.005
3	2 (22)	1 (8)	0.54
4	2 (22)	12 (92)	0.0015
Extent of surgery			
Biopsy	2 (22)	2 (15)	>0.99
PR	2 (22)	5 (38.5)	0.65
STR	1 (11)	0 (0)	0.41
GTR	2 (22)	3 (23)	>0.99
Treatment			
Surgery	7 (77.8)	10 (77)	>0.99
Surgery + RTx	2 (22.2)	8 (61.5)	0.07
Surgery + CTx	2 (22.2)	9 (69)	0.03
Surgery + RTx + CTx	1 (11)	8 (61.5)	0.02
Other Tx*	2 (22.5)	6 (46)	0.38
Leptomeningeal spread	2 (25)	6 (46)	0.27
Level of lesion			
Infratentorial	0 (0)	3 (23)	0.26
Cervical	5 (62.5)	6 (46.2)	0.66
Thoracic	4 (50)	5 (38.5)	0.67
Lumbar	1 (12.5)	1 (7.6)	>0.99

Data are shown as mean ± standard deviation or number of patients and (%).
*Other therapies included IVIG, Nivolumab, Avastin, Crisotinib, Binimetinib, Zarnestra, Temozolomide, Vinblastine, Trametinib, and Everolimus.

Radiological Analysis

Sixteen of the 22 patients had preoperative imaging available. In 12 (75%), the tumor had areas of enhancement and 2 (12.5%) demonstrated surrounding cord T2 hyperintensity, suggesting edema. Out of the 12 patients with enhancement, 9 (75%) were K27M-mutant tumors ($p = 0.01$). Of the 16 patients with imaging, 7 had progression of disease. Tumor length varied from 2-segments to 6-segments long. Out of the 7 patients with disease progression, 5 (71%) were K27M-mutant tumors with enhancement. The K27M-mutant tumors were long-segmental lesions, the longest involving the cervicomedullary junction extending to C6. Eight patients had extensive leptomeningeal enhancement at the time of diagnosis (Fig. 2). Of those with leptomeningeal disease, 75% were K27M-mutant tumors; however, the difference did not reach statistical significance ($p = 0.27$).

Histology and Immunohistochemistry

Histopathologically, patients diagnosed with H3-wildtype tumors showed a lower histological grade (2.75 ± 0.82) compared to those diagnosed with H3 K27M-mutant tumors (3.9 ± 0.27) ($p = 0.0004$). The youngest patient with a spinal cord GBM was 2 years old. There were 11 (50%) tumors classified by histology as GBM (100% K27M-mutant), 4 (18%) anaplastic astrocytoma WHO 3 (50% K27-altered), and 7 (32%) diffuse astrocytomas WHO 2 (0% K27-altered). K27M-mutant tumors showed a wide variety of histological features, ranging from diffuse SCG with mildly increased cellularity and atypia, to classic glioblastoma with microvascular proliferation and pseudopalisading necrosis as well as extreme nuclear pleomorphism (Fig. 3).

Histone H3 K27M mutation was tested by IHC (15 cases) and/or DNA methylation array (16 cases). Of the 22 tumors, 13 (59%) were positive for the histone H3 K27M mutation, 2 (9%) pilocytic astrocytoma, and 1 (4.5%) glioblastoma

Downloaded from https://academic.oup.com/jnen/advance-article/doi/10.1093/jnen/nlac075/6673886 by New York University Law School Library user on 15 September 2022

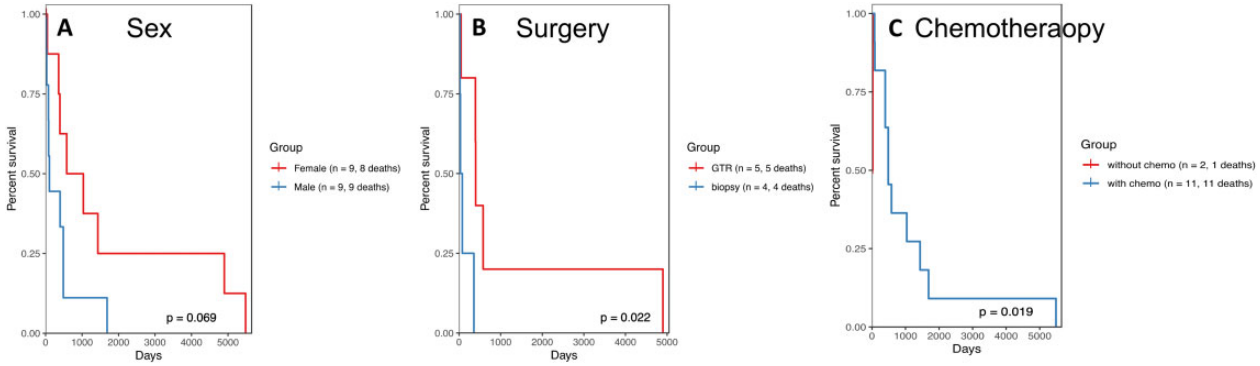

FIGURE 1. Kaplan-Meier curves showing overall survival of H3-wildtype and K27-altered tumors in our cohort. **(A)** Overall survival curve based on sex. Decreased overall survival was observed in male compared to females ($p = 0.069$). **(B)** Overall survival curve-based surgery type. Decreased overall survival was observed in the biopsy group compared to the gross total resection (GTR) group ($p = 0.022$). **(C)** Overall survival curve based on chemotherapy. A trend toward decreased overall survival for K27-altered tumors was observed ($p = 0.1$).

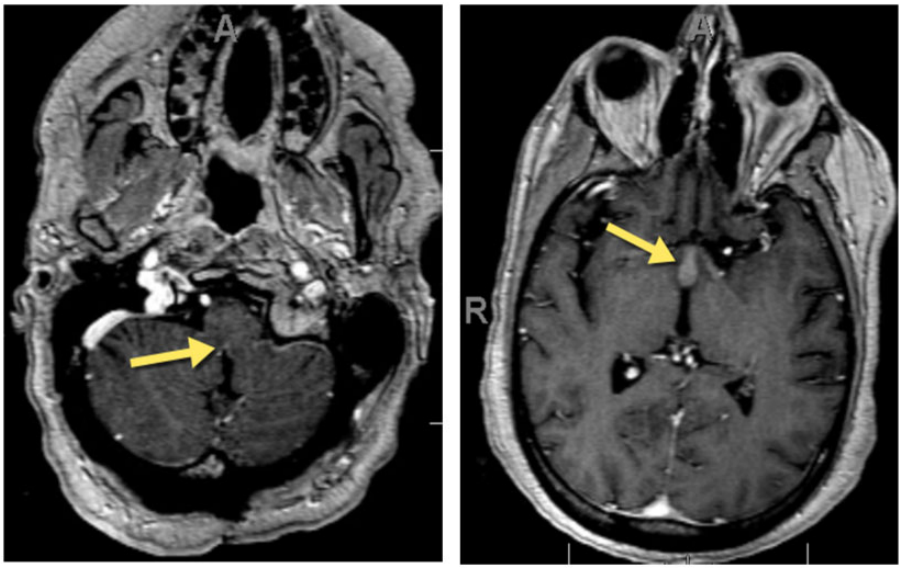

FIGURE 2. Patient with K27-altered tumor with leptomeningeal disease, as highlighted by the arrows, at the time of diagnosis.

IDH-wildtype either by IHC or DNA methylation. The K27M mutation was nearly equally prevalent in the cervical (54%) and thoracic (46%) spinal cord. Interestingly, both K27-wildtype tumors as well as the K27M-mutant tumors were present in adult (11, 55% K27M-mutant) and pediatric populations (11, 73% K27M-mutant) and the histone H3 K27M mutation was the single most prevalent aberration we could identify and was present in 55% of adult and 64% of pediatric tumors. All tumors that harbored the K27M mutation were high-grade tumors, while only 44% of the wildtype tumors were high grade (Table). All tumors were negative for the BRAF V600E and IDH1 R132H mutations and none classified as IDH mutant glioma, or any of the methylation low-grade glioma subclasses by DNA methylation. In the 16 tumors with MGMT promoter methylation tested, the MGMT promoter of 10 K27M-mutant tumors were unmethylated, while the rest were methylated K27-wildtype tumors.

DNA Methylation Analysis and Copy Number Changes

Copy number profiles from the DNA methylation array showed that K27M-mutant tumors have complex copy number changes with multiple large chromosomal gains and losses compared to H3 K27-wildtype tumors (Fig. 4). In contrary, H3 K27-wildtype tumors were characterized by lack of significant copy number changes. In H3 K27M-mutant tumors, copy number varied from almost no changes, to extensive gains and losses of whole chromosomes across the genome. K27M-mutant tumors with chromosomal aberrations included

Downloaded from https://academic.oup.com/jnen/advance-article/doi/10.1093/jnen/nlac075/6673886 by New York Universtiy Law School Library user on 15 September 2022

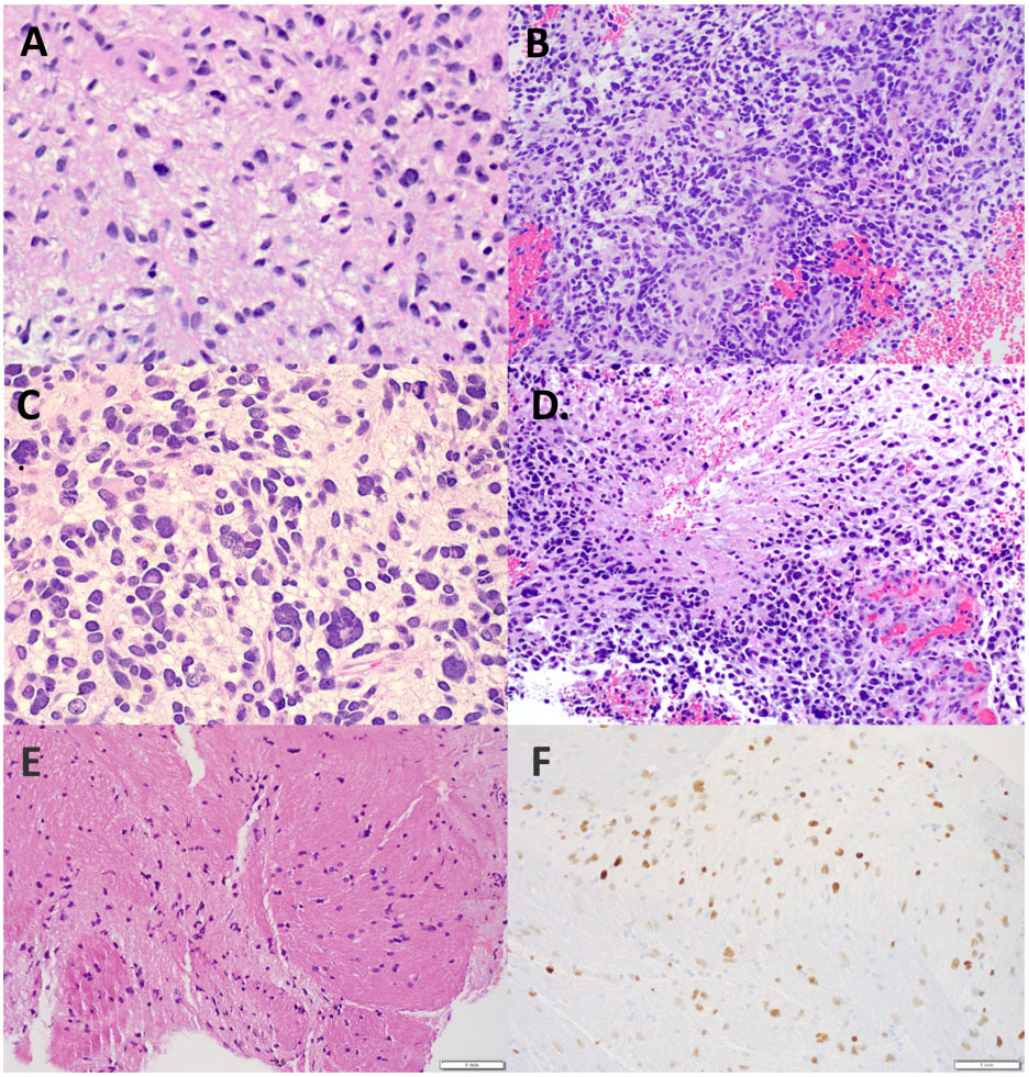

FIGURE 3. K27-altered tumors stained with hematoxylin and eosin (H&E). Tumors had a wide variety of histological features. **(A)** Mildly hypercellular with mild-moderately pleomorphic cells, **(B)** hypercellular with small round blue cells, **(C)** hypercellular with severely pleomorphic cells some of which are multinucleated, **(D)** hypercellular with microvascular proliferation and pseudopalisading necrosis, **(E)** a hypocellular lesion with mildly pleomorphic tumor cells and the concurrent immunostain **(F)** H3 K27M.

chromosome 13 loss (including *Rb* gene) and chromosome 17 loss (including *NF1*, *TP53* genes) and focal amplifications of receptor kinase genes *MET* and *PDGFRA* as is commonly observed in adult classic hemispheric GBMs. One of the pediatric (6-years old) and adult (58-years old) patients with H3 K27M-mutant tumor showed homozygous loss of *NF1* locus. A DNA methylation hierarchical clustering showed distinct methylation patterns between K27-wildtype and K27M-mutant tumors (Fig. 5).

DISCUSSION

The molecular characteristics of cerebral hemispheric gliomas have been extensively studied. In contrast, the available molecular features of diffuse SCG are few to date, largely due to both their rarity and limited availability of tissue. In this study, we analyzed the clinical and pathological characteristics as well as the molecular features of 22 diffuse SCGs in both adult and pediatric patients.

Prior studies of cerebral H3 K27M-mutant gliomas have suggested a trend for male predominance (19–21). Our study showed a significant male predominance for the K27M-mutant tumors compared to H3 K27-wildtype ($p < 0.05$). This is unusual as other frequent molecular drivers of gliomas such as *IDH1/2*, *BRAF*, or *EGFR* do not appear to show sex preference. The biological mechanism of why K27M is more prevalent in male diffuse SCG is currently not known.

There is no current standard of therapy for diffuse SCG. The most common treatment available is a trimodal therapy consisting of maximal safe surgical resection, radiation, and

Downloaded from https://academic.oup.com/jnen/advance-article/doi/10.1093/jnen/nlac075/6673886 by New York University Law School Library user on 15 September 2022

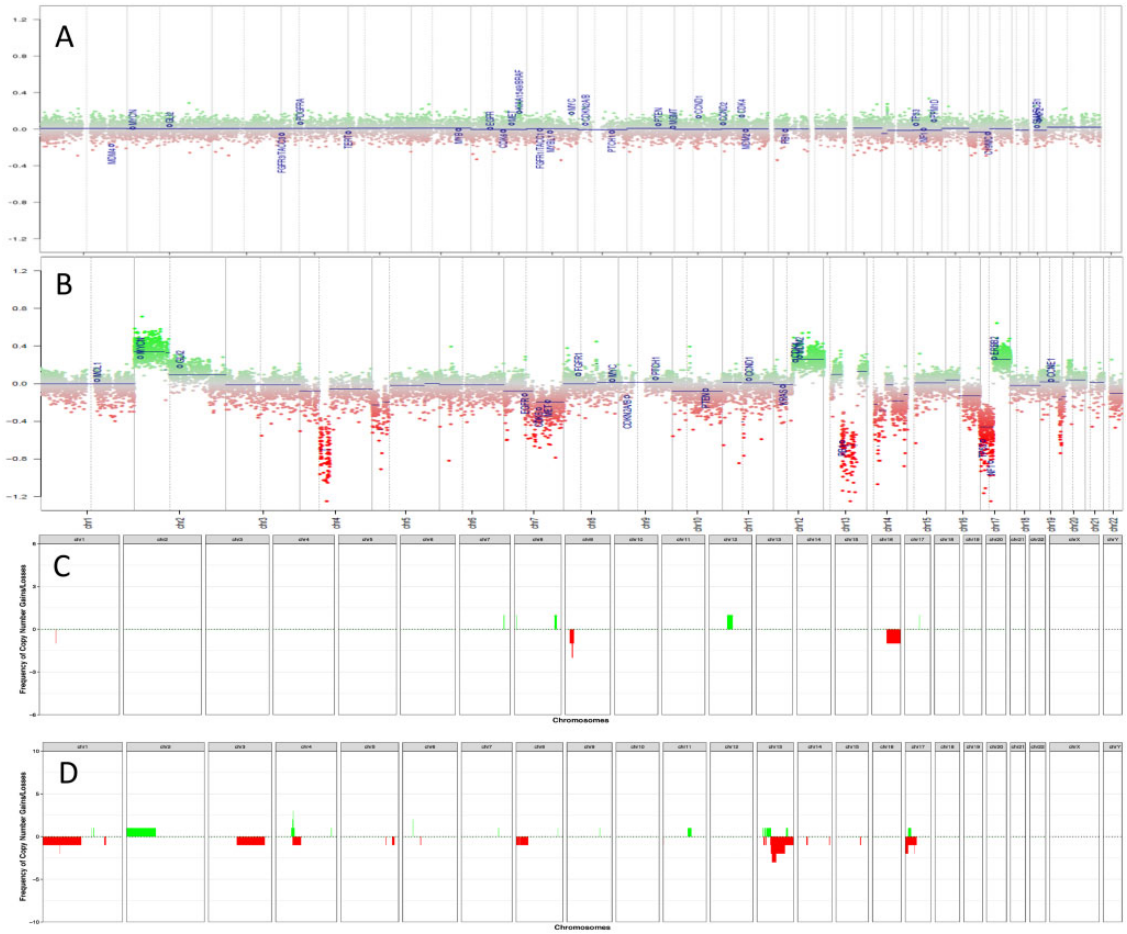

FIGURE 4. Genome-wide copy number profiles generated by DNA methylation data of a representative wildtype **(A)** and K27-altered tumor **(B)**. Cumulative copy number profiles show K27-altered tumors **(D)** with increased copy number variation compared to wildtype tumors **(C).**

chemotherapy. In our study, there was an overall decreased survival in the biopsy cohort compared to those who received GTR ($p = 0.022$), suggesting that attempt for maximum safe resection has the largest impact on survival. In our cohort, patients not receiving chemotherapy showed decreased overall survival compared to those who did ($p = 0.019$). The most commonly used chemotherapy agent in our cohort was temozolomide. Other therapies included binimetinib, avastin, and ONC201. Finally, radiation was not associated with improved overall survival ($p = 0.772$), suggesting a limited role of radiation in spinal cord malignant gliomas compared to surgery and chemotherapy.

Qiu et al recently published their imaging findings of H3 K27M-mutant tumors in which they described the majority of tumors as contrast-enhanced, solid tumors with uniform signals on MRI with rare edema and hemorrhage (19). In our study, 75% of the contrast-enhancing tumors were K27M-mutant ($p = 0.04$). In agreement with Qiu et al, only 2 K27M-mutant tumors in our study had surrounding edema; however, presurgery imaging was not available for all patients (19). It is reasonable to assume that spinal high-grade gliomas would have a predilection for widespread disease given that spinal low-grade gliomas also have a high rate of disease progression (22).

The reported incidence of the H3 K27M mutation in diffuse SCG has varied over the years. Recent studies such as from Solomon et al have reported a rate of 53% ($n = 9/17$) for K27M in both adult and pediatric patients, while Picca et al and Karremann et al reported rates of 62.5% and 54% ($n = 6/11$), respectively, in adult patients (23–25). In our cohort of adult and pediatric patients, we found an incidence of 59% H3 K27M-mutant gliomas ($n = 13$), making it the single most prevalent driver. Diffuse midline gliomas harboring the H3 K27M mutation are known to carry a dismal prognosis (22, 25–27). Although we found no significant survival difference between H3 K27M-mutant and wildtype spinal tumors ($p = 0.366$) in our cohort, this finding might be attributable to our low sample number and limited follow-up data.

The differences in molecular characteristics of the different subtypes of diffuse SCG are not well established. K27M mutation induces a markedly distinct DNA methylation signature, which can be used for diagnostics by DNA methylation array. In our study, K27M-mutant tumors showed a large variety of histological features with histological features ranging

Downloaded from https://academic.oup.com/jnen/advance-article/doi/10.1093/jnen/nlac075/6673886 by New York University Law School Library user on 15 September 2022

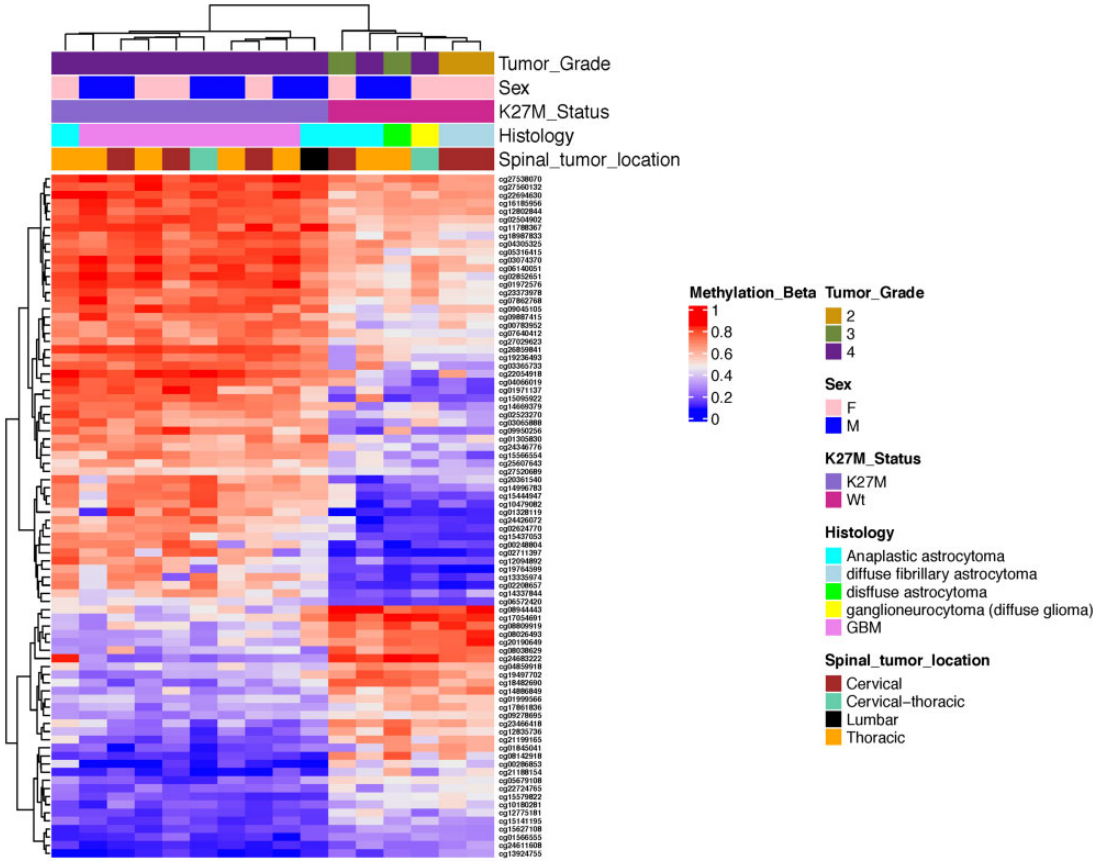

FIGURE 5. Heatmap of DNA methylated regions of spinal cord glioma samples using the top 84 most differentially methylated probes. Hierarchical supervised clustering was based on disease presence K27M mutation status. Methylation beta-values are illustrated based on the color scale.

from low- to high-grade tumors. Our results show that diffuse SCG have distinct molecular profiles and markedly increased levels of CNV s of K27M-mutant tumors compared to H3 K27-wildtype tumors, with gains of chromosomes 2 and 4 and loss of chromosomes 1, 3, 13, and 17.

Our study suggests that diffuse SCG can be divided into at least 2 molecularly distinct groups. The first is characterized by K27M mutation, distinct epigenetic phenotype, chromosomal instability, and male predominance, and the second is characterized by K27-wildtype, often histologically lower grade, with few chromosomal aberrations. Further studies are necessary to characterize the molecular profile of the H3 K27-wildtype tumors and to understand how molecular differences can translate into improved treatment of these diseases.

ACKNOWLEDGMENTS

The DNA methylation profiling was in part supported by grants from the Friedberg Charitable Foundation and the Making Headway Foundation (to MS).

REFERENCES

1. Schellinger KA, Propp JM, Villano JL, et al. Descriptive epidemiology of primary spinal cord tumors. J Neurooncol 2008;87:173–9
2. Chamberlain MC, Tredway TL. Adult primary intradural spinal cord tumors: A review. Curr Neurol Neurosci Rep 2011;11:320–8
3. Minehan KJ, Brown PD, Scheithauer BW, et al. Prognosis and treatment of spinal cord astrocytoma. Int J Radiat Oncol Biol Phys 2009;73:727–33
4. Henson JW. Spinal cord gliomas. Curr Opin Neurol 2001;14:679–82
5. Shrivastava RK, Epstein FJ, Perin NI, et al. Intramedullary spinal cord tumors in patients older than 50 years of age: Management and outcome analysis. J Neurosurg Spine 2005;2:249–55
6. Zhang M, Iyer RR, Azad TD, et al. Genomic landscape of intramedullary spinal cord gliomas. Sci Rep 2019;9:18722
7. Townsend N, Handler M, Fleitz J, et al. Intramedullary spinal cord astrocytomas in children. Pediatr Blood Cancer 2004;43:629–32
8. Chai RC, Zhang YW, Liu YQ, et al. The molecular characteristics of spinal cord gliomas with or without H3 K27M mutation. Acta Neuropathol Commun 2020;8:40
9. Abd-El-Barr MM, Huang KT, Moses ZB, et al. Recent advances in intradural spinal tumors. Neuro Oncol 2018;20:729–42
10. Brat DJ, Aldape K, Colman H, et al. cIMPACT-NOW update 3: Recommended diagnostic criteria for "Diffuse astrocytic glioma, IDH-wildtype, with molecular features of glioblastoma, WHO grade IV". Acta Neuropathol 2018;136:805–10
11. Sloan EA, Cooney T, Oberheim Bush NA, et al. Recurrent non-canonical histone H3 mutations in spinal cord diffuse gliomas. Acta Neuropathol 2019;138:877–81
12. Mosaab A, El-Ayadi M, Khorshed EN, et al. Histone H3K27M mutation overrides histological grading in pediatric gliomas. Sci Rep 2020;10: 8368
13. Zhang P. Clinical, radiological, and pathological features of 33 adult unilateral thalamic gliomas. Word J Surg Oncol 2016;14:78
14. Tang K, Kurland D, Vasudevaraja V, et al. Exploring DNA methylation for prognosis and analyzing the tumor microenvironment in pleomorphic xanthoastrocytoma. J Neuropathol Exp Neurol 2020;79:880–90

Downloaded from https://academic.oup.com/jnen/advance-article/doi/10.1093/jnen/nlac075/6673886 by New York University Law School Library user on 15 September 2022

15. Aryee MJ, Jaffe AE, Corrada-Bravo H, et al. Minfi: A flexible and comprehensive bioconductor package for the analysis of Infinium DNA methylation microarrays. Bioinformatics 2014;30:1363–9
16. Gu Z, Eils R, Schlesner M. Complex heatmaps reveal patterns and correlations in multidimensional genomic data. Bioinformatics 2016;32:2847–9
17. Hovestadt V, Zapatka M. conumee: Enhanced copy-number variation analysis using Illumina DNA methylation arrays. Available at: https://rdrr.io/bioc/conumee/
18. Skidmore ZL, Wagner AH, Lesurf R, et al. GenVisR: Genomic visualizations in R. Bioinformatics 2016;32:3012–4.
19. Qiu T, Chanchotisatien A, Zhiyong Q, et al. Imaging characteristics of adult H3 K27M-mutant gliomas. J Neurosurg 2019;133:1662–70
20. Buczkowicz P, Hoeman C, Rakopoulos P, et al. Genomic analysis of diffuse intrinsic pontine gliomas identifies three molecular subgroups and recurrent activating ACVR1 mutations. Nat Genet 2014;46:451–6
21. Sun T, Plutynski A, Ward S, et al. An integrative view on sex differences in brain tumors. Cell Mol Life Sci 2015;72:3323–42
22. Perwein T, Benesch M, Kandels D, et al. High frequency of disease progression in pediatric spinal cord low-grade glioma (LGG): Management strategies and results from the German LGG study group. Neuro Oncol 2021;23:1148–62
23. Solomon DA, Wood MD, Tihan T, et al. Diffuse midline gliomas with histone H3-K27M mutation: A series of 47 cases assessing the spectrum of morphologic variation and associated genetic alterations. Brain Pathol 2016;26:569–80
24. Picca A, Berzero G, Bielle F, et al. *FGFR1* actionable mutations, molecular specificities, and outcome of adult midline gliomas. Neurolology 2018;90:e2086–94
25. Karremann M, Gielen GH, Hoffmann M, et al. Diffuse high-grade gliomas with H3 K27M mutations carry a dismal prognosis independent of tumor location. Neuro Oncol 2018;20:123–31
26. Khuong-Quang DA, Buczkowicz P, Rakopoulous P, et al. K27M mutation in histone H3.3 defines clinically and biologically distinct subgroups of pediatric diffuse intrinsic pontine gliomas. Acta Neuropathol 2012;124:439–47
27. Lu VM, Alvi MA, McDonald KL, et al. Impact of the H3K27M mutation on survival in pediatric high-grade glioma: A systematic review and meta-analysis. J Neurosurg Pediatr 2019;23:308–16

Downloaded from https://academic.oup.com/jnen/advance-article/doi/10.1093/jnen/nlac075/6673886 by New York Universtiy Law School Library user on 15 September 2022